Annales Societatis Geologorum Poloniae (2009), vol. 79: 53–66.

PROVENANCE AND DIAGENESIS OF SILICICLASTIC AND ORGANIC MATERIAL IN THE ALBIAN–TURONIAN SEDIMENTS (SILESIAN NAPPE, LANCKORONA, OUTER CARPATHIANS, POLAND): PRELIMINARY STUDIES

Patrycja WÓJCIK-TABOL & Andrzej ŚLĄCZKA

Institute of Geological Sciences, Jagiellonian University, Oleandry 2a, 30-063 Kraków, Poland, e-mails: p.wojcik-tabol@uj.edu.pl, slaczka@ing.uj.edu.pl

Wójcik-Tabol, P. & Ślączka, A., 2009. Provenance and diagenesis of siliciclastic and organic material in the Albian–Turonian sediments (Silesian Nappe, Lanckorona, Outer Carpathians, Poland): preliminary studies. *Annales Societatis Geologorum Poloniae*, 79: 53–66.

Abstract: The provenance and diagenesis of the siliciclastic and hemipelagic sediments of three lithostratigraphic units: Lhoty Formation, Barnasiówka Radiolarian Shale Formation (BRSF) and Variegated Shales from Lanckorona area, Polish Outer Carpathians, was approached by means of petrological and geochemical analysis of the representative samples. Data show that studied succession was mainly derived from two sources: 1. a dominant terrigenous fine-grained components have affinity with average upper continental crust (basing on mineral detritus, K_2O/Rb ratio and Y/Ni vs. Cr/V ratios) and 2. biogenic siliceous material and macerals. Composition varies up section and accounts for changes in the detrital supply due to eustatic sea-level changes. Organic petrology shows presence of organic detritus within the Lhoty Fm and dominance of marine-derived macerals in the BRSF. Chemical and petrological features imply a progressive deepening of the basin. The studied succession was diagenetically altered (*e.g.* coalification of bituminite, illitisation of smectite and pyritisation).

Key words: organic and inorganic geochemistry, Albian–Turonian, Silesian Nappe, Outer Carpathians, Poland.

Manuscript received 1 October 2007, acceepted 16 April 2009

INTRODUCTION

The Outer Carpathian basins were situated during Cretaceous times between the converging European continent and the Inner Carpathian plate (Oszczypko, 1999; Golonka *et al.* 2000, 2008b). During its opening and post-rift subsidence (Late Jurassic–Early Cretaceous), the Silesian Basin was filled with calcareous turbidites followed by siliciclastic turbidites and hemipelagic shales (Oszczypko 2004). The siliciclastic and biogenic materials were supplied from two main sources: the European Platform and the Silesian Cordillera (*e.g.*, Wieser, 1948; Burtan *et al.*, 1984; Bąk, 2007b).

During the Albian–Cenomanian (Gedl, 2001; Bąk *et al.*, 2005, Golonka *et al.*, 2008b) turbidite complexes of the Lhoty Formation were deposited in the axial part of the basin. A low and decreasing rate of sedimentation (20–40 m/My) was characteristic for the Silesian Basin (Poprawa *et al.*, 2002). The Lhoty Formation deposition took place during relatively low sea level and was controlled by a post-rift thermal subsidence (Poprawa *et al.*, 2002; Nemčok *et al.*, 2001). The Barnasiówka Radiolarian Shale Formation (BRSF) is developed as the green radiolarian shales and radiolarites, intercalated with black shales containing bentonites and ferro-manganiferous concretions and layers (Książkiewicz 1951; Koszarski & Ślączka, 1973; Bąk *et al.*, 2001; Bąk, 2006, 2007a–d). The BRSF was deposited during the Late Cenomanian–Early Turonian under high-stand sea level condition (Bąk, 2007a). It is overlain by the Turonian Variegated Shales (VS) that represent a product of deep-sea hemipelagic sedimentation (Koszarski & Ślączka, 1973). The hydrothermal activity could develop during the Albian maximal extension of continental crust and lasted at least through the Turonian (Burtan & Turnau-Morawska, 1978; Gucwa & Wieser, 1978; Geroch *et al.*, 1985; Bąk, 2006, 2007a–d).

The present paper shows results of mineralogical and geochemical investigation of hemipelagic sediments to indicate the provenance of the mineral and organic detritus and diagenetic changes of the sediment. Pelagic sediment formation is affected by many processes, including detrital supply from continental areas as well as hydrothermal and biological activity, and diagenesis (Chester, 1990). Chemical records of the environmental changes across the Ceno-

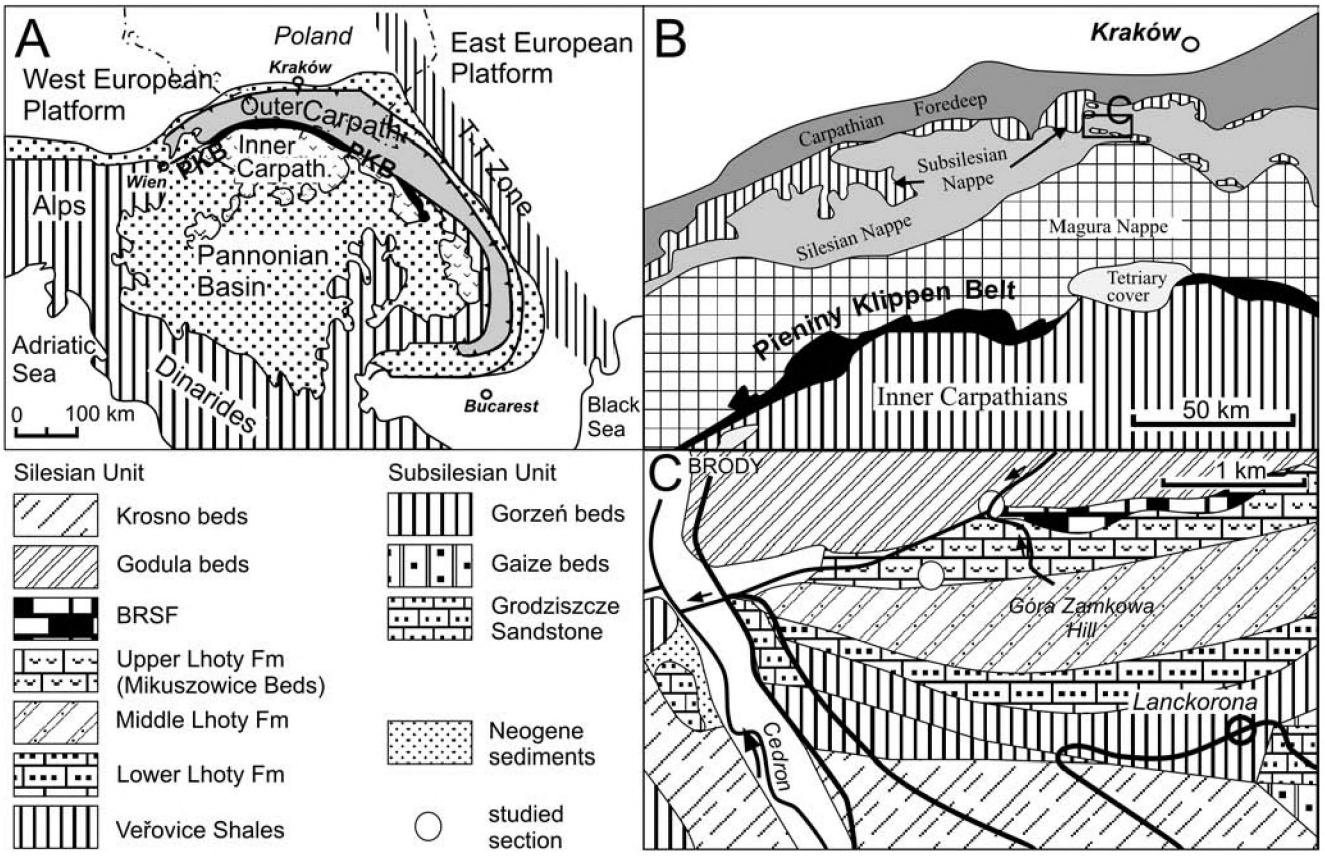

Fig. 1. Location of the studied area at the background of main geological units: **A.** Simplified tectonic scheme of the Alpine orogens; PKB – Pieniny Klippen Belt (after Kovač *et al.*, 1998, modified); **B.** Central part of Polish Carpathians (after Żytko *et al.*, 1989); C. Detailed division of the Silesian and Subsilesian units in the Lanckorona region (after Książkiewicz, 1977)

manian–Turonian transition in the Polish Carpathians were presented earlier by Bąk (2006, 2007a–d). The main objectives of this study is presentation of new data with correlation to that previous.

GEOLOGICAL SETTING

The Polish Carpathians are part of the great arc of mountains stretching for more than 1300 km. The Polish part of the Outer Carpathians consists of stacked nappes and thrust-sheets, such as the Subsilesian, Silesian, Skole, Dukla and Magura Nappes (Fig. 1; Książkiewicz, 1977).

The presented paper concerns the sediments of the Silesian Nappe, which were deposited in the Subsilesian–Silesian Basin (Severinic-Moldavidic *sensu* Ślączka, 2006) from Late Albian to Early Turonian (Książkiewicz, 1962). The samples represent siliciclastic and hemipelagic sediments of three lithostratigraphic units: turbiditic Lhoty Formation (*sensu* Golonka *et al.*, 2008a, previously known as Lgota Beds, e.g. Bieda *et al.*, 1963), Barnasiówka Radiolarian Shale Formation (BRSF; *sensu* Bąk *et al.*, 2001) and Variegated Shales.

The section studied is located in western part of the Silesian Nappe, within the Lanckorona Foothills, about 30 km south-west from Kraków (Fig. 1). The main outcrop is situated in the banks of a small creek, a right tributary of the Cedron stream. This section is small and strongly folded. The studied succession appears in reverse order and contains numerous tectonic hiatuses.

The oldest sediments exposed in the northern part of studied section belong to the Barnasiówka Radiolarian Shale Formation. They are represented by black and green, siliceous shales (Fig. 2E) with intercalations of bentonites and ferromanganese horizons (up to 5 cm thick) (Figs 2C, D; 5A). The thickness of these strata amounts to about 5 m. Further, upwards the succession a complex of red and greenish grey thin- and medium-bedded siliceous shales with thin intercalations of glauconitic sandstones and greenish cherts is exposed (Fig. 2A, B). This part is about 3.8 m thick and belongs to the Upper Cretaceous Variegated Shales.

When going towards the south, upward the hill, the old quarries of the Middle and Upper Lhoty Formation occur. The Middle Lhoty Formation consists mostly of thin-and medium-bedded siliceous dark-grey sandstones. They are interbeded with black, grey and spotty, lightly-calcareous shales (Fig. 3A–D). The upper division of the Lhoty Formation, named the Mikuszowice Chert Member (Szajnocha, 1884 in Golonka *et al.* 2008b; Bieda *et al.*, 1963) is represented by medium- and thick-bedded (about 50 cm) sandstones with bluish cherts in the middle and upper parts of layers intercalated with grey and black shales (Fig. 4A, B).

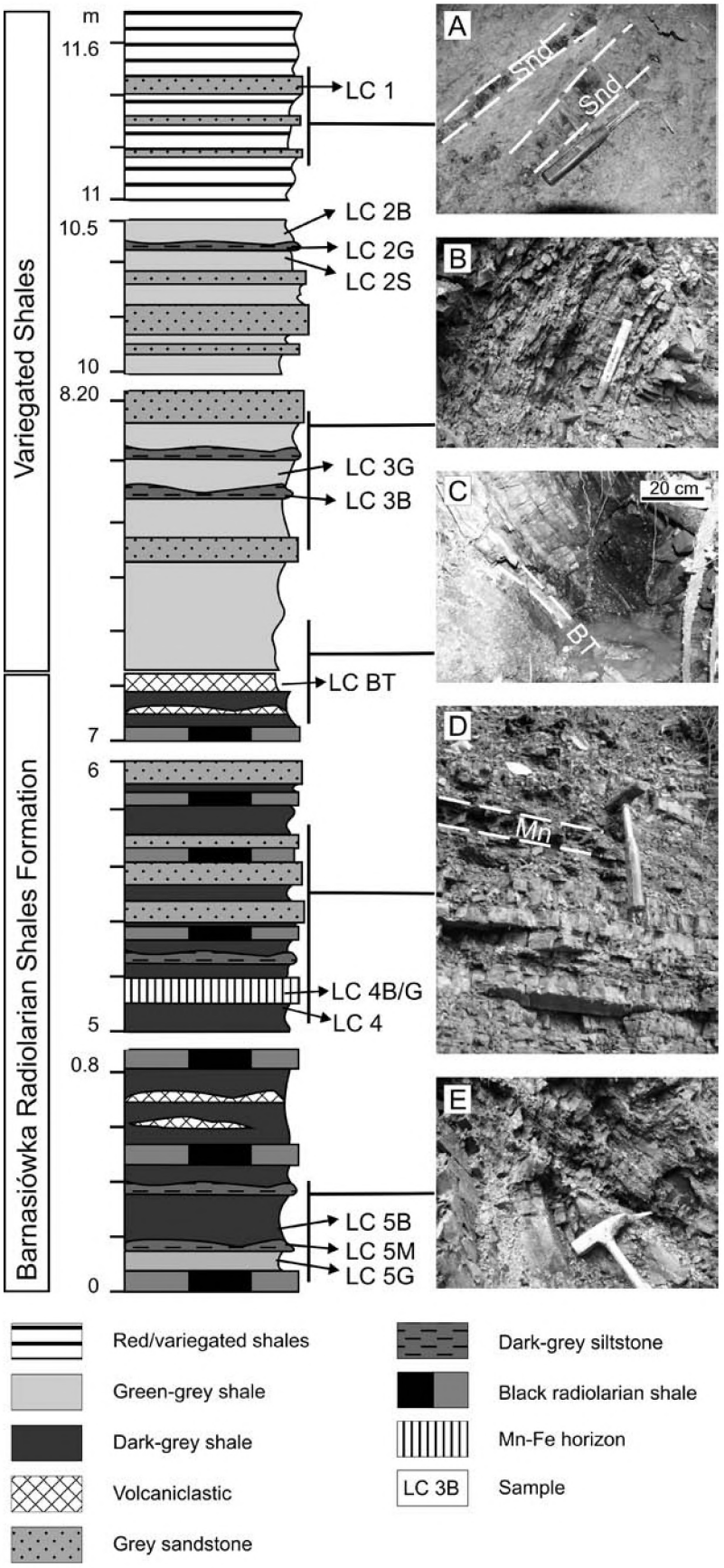

Fig. 2. Lithological log of the Lanckorona section. Variegated Shales: **A.** Red and greenish-grey, thin- and medium-bedded siliceous shales with glauconitic sandstone (Snd); **B.** Sequence of green-grey shales interbedded by quartzitic sandstone; Barnasiówka Radiolarian Shale Formation: **C.** Bentonite (BT) intercalation within none-calcareous black and green shales; **D.** Organic-rich shales and radiolarites with Mn-Fe horizon (Mn); **E.** Siliceous black and green shales with intercalation of volcanoclastic layers

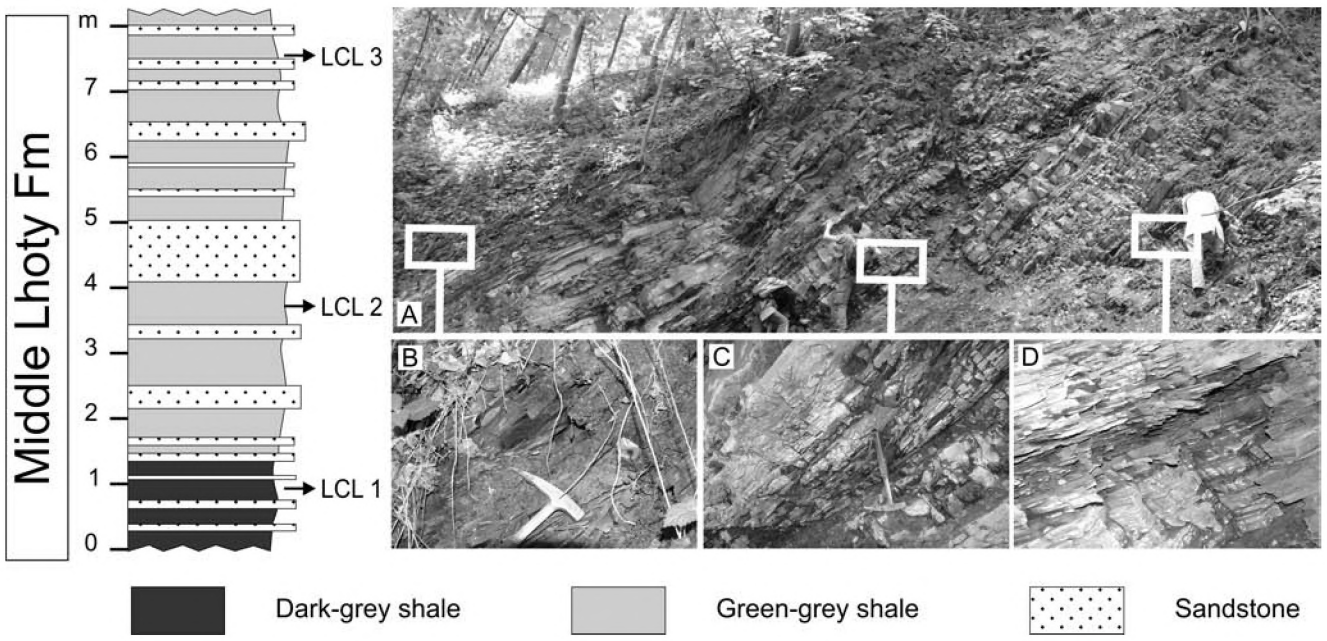

Fig. 3. The Middle Lhoty Formation; A–D. Thin- and medium-bedded siliceous dark-grey sandstone interbedded with black, grey and spotty, low-calcareous shales

MATERIALS AND METHODS

Microstructures and organic petrological indices in 15 samples using microscopic observation (Nicon ECLIPSE, E 600 POL; transmitted and reflected light) were examined.

The samples were studied by X-ray diffraction (XRD) both as bulk rocks and in <0.2 μm fractions separated from these rocks. The pelitic fractions <0.2 μm were separated using the complete Jackson (1975) procedure, applied in order to dissolve carbonates and remove organic matter and iron oxides. They were studied as oriented preparations, sedimented on glass slides, both in air- dry and ethylene glycol saturated form. A Philips diffractometer, equipped with a Cu lamp, and a monochromator were used.

The identification of clay minerals followed the method outlined by Moore and Reynolds (1997). Mixed-layer illite-smectite and smectite were identified in glycolated preparations using the positions of appropriate pairs of basal reflections (Środoń, 1980, 1984; Dudek & Środoń, 1996).

The amounts of major oxides were determined in 15 samples using an inductively coupled plasma – optical emission spectrometry (ICP-OES). Trace-element were determined by the inductively coupled plasma – mass spectroscopy (ICP-MS) using a Perkin Elmer Elan 6000 ICP at the ACME Analytical Laboratories, LTD, in Vancouver, Canada.

The enrichment factors (EF) for major and trace elements relative to the Post-Archean Australian Shale (PAAS, Taylor & McLennan, 1985) were used in the discussion. The values of enrichment factor are calculated as follows (* according to Taylor & McLennan (1985):

(element content/Al content) $_{sample}$ */(element content / Al content)* $_{PAAS}$*

RESULTS

MINERALOGY AND PETROLOGY

The XRD patterns of whole-rock analysed samples show that, in general, they (Lhoty Formation, BRSF and Variegated Shales) are rich in quartz, associated with clay minerals, and contain small amounts of feldspar. Calcite is present in the Lhoty Formation samples and rarer within shales of the BRSF, absent in the Variegated Shales.

Upward the succession, from the Middle Lhoty Formation through the Variegated Shales, the quartz content increases. The clay mineral composition varies slightly and consists mainly of illite and mixed layers illite/smectite (I/S). The content of illitic layers in the I/S range between 10 and 60%. The Lhoty Fm. siltstones contain the lowest amounts of smectite, while the clayey shales of the BRSF are enriched in it. The highest amounts of smectite occur within the volcanoclastic layers in the BRSF (about 80%). Kaolinite is the associating clay mineral in the shales of the Middle Lhoty Fm. Upward the section, kaolinite content decreases. It finally disappears in the lower part of the Variegated Shales. Chlorite has been recognized in minor amount within the Middle Lhoty Formation only.

Observations of thin-section of green-grey shales (within both: Lhoty Formation and BRSF) reveal the wavy- and parallel lamination (Fig. 5D). The ichnofossils are also noted (Fig. 5B). The burrows are enriched in organic matter, which is usually associated with pyrite. Pyrite occurs as massive, anhedral grains. Radiolaria and sponge spicules have been there often recognised. Tests are oriented parallel to the bedding. The single grains of glauconite, quartz, mica and organic detritus (cell-structured macerals, e.g. semifusinite) are dispersed within argillaceous matrix.

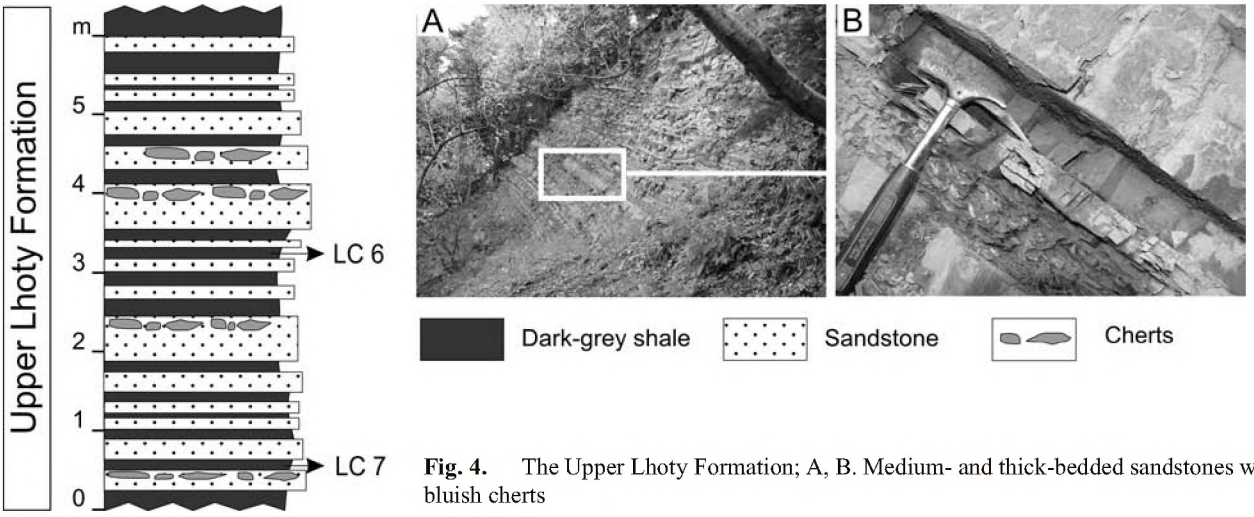

Fig. 4. The Upper Lhoty Formation; A, B. Medium- and thick-bedded sandstones with bluish cherts

The parallel lamination occurs within black shales (within both: Lhoty Formation and BRSF). It is emphasised by abundant organic matter (Fig. 5C) represented by a dark, amorphous substance and terrestrial detritus (Fig. 5E–H). The samples include very rare radiolarian tests as the only biotic component. Pyrite occurs as very thin framboids and crystals. The size of both varies from 5 to 12 μm, where predominately 8 – 10 μm in diameter (Fig. 5E, H).

The manganiferous horizon, 2–5 cm thick occurs within the siliceous shales of the BRSF. It overlies the package of black and green clayey shales with bentonite intercalation. The Mn-Fe layer contains many concentrically zoned nodules that are less than 3 cm in size. The nodules are built of greenish core and outer black rim (Fig. 6A). The thin-section images exhibit the presence of numerous rhombohedric pseudomorphs (50 μm in size on average) dispersed within silica (cryptocrystalline chalcedony) admixed with clay minerals matrix (Fig. 6B). In the internal part of the nodules, silica adopts rhombohedral shape whereas rhombohedra of the outer crust are infilled by the Fe and Mn oxy-hydroxides (Fig. 6C, E). The pseudomorphs from the external part of the nodules contain massive aggregates of pyrite (Fig. 6D).

The studied Variegated Shales overlying the BRSF are represented by siliceous red and green shales with thin-bedded sandstones. The shales are clayey, barren of detritus. The fine-grained intercalations consist of quartz, mica, feldspars and glauconite. Some sandstone layers are enriched in Fe-Mn oxy-hydroxides.

GEOCHEMISTRY

The relatively low amounts of the major oxides (Fe_2O_3 and MnO, MgO, CaO, TiO_2, Na_2O, K_2O) have been determined in the samples studied (Tab. 1). Their amounts are lower (occasionally similar) than that in PAAS. Only SiO_2 contents are well above the SiO_2 content of PAAS (62.8 wt. %; Taylor & McLennan, 1985). The amount of silica in the selected samples of the BRSF and Variegated Shales is higher than in others. The manganiferous sample (LC 4BG), despite its low SiO_2 content (43.82 wt. %) has a high SiO_2 (2.83) enrichment factor (EF) because of low Al_2O_3 content (4.66 wt. %).

In the SiO_2 vs. Al_2O_3 diagram (Fig. 7), the studied samples display negative correlation between these oxides. The majority of samples show similar SiO_2/Al_2O_3 ratio (5 in average, without manganiferous samples). They are located in a small field approximately along one trend-line. The exception is Fe-Mn sample (LC 4BG) that is out of general direction due to low content of SiO_2 and Al_2O_3.

MnO, P_2O_5, Y, La, Ce

The distributions of these elements are irregular (Tab. 1; Fig. 8). The Lhoty Formation seem to be more enriched in upper part than in lower – it might be connected with lithology. The most enriched samples from the Upper Lhoty Formation contain abundant detritus.

In general, itrum contents vary between 13.2 and 39 ppm in the samples studied, whereas in the PAAS it yields 27 ppm. Therefore, $(EF)_Y$ values vary from 0.65 to 5.87. The manganiferous sample (LC 4BG) is the most enriched in Y. The high Y concentration was also noted in the Mn-rich sandstone of the Variegated Shales (LC 1).

The La contents differ within narrow range; they equal to 30 ppm in average, with maximum in the volcanoclastic samples (LC BT). Nevertheless, the highest values of enrichment factor are noted in the LC 1 and LC 4BG samples (EF are 2.58 and 3.36).

The absolute contents of cerium are low with a small rise in the Mn-rich LC 4BG and ?volcanoclastic (LC BT) samples from the BRSF. The enrichment factor variety shows similar pattern like La and Y. Their values do not exceed unity, except of the LC 4 BG and LC 1, where EF amounts to 3 and 6.37 respectively. Worth to note that elevation of the EF values in both samples is affected by low percentage of Al_2O_3.

The enrichment of Y, La and Ce correlates with increasing concentrations of MnO and P_2O_5. The BRSF and Variegated Shales are enriched of MnO and P_2O_5 obviously. The highest content of oxides characterises the LC 4BG and LC 1 sample. The LC 4B and LC 3 samples exhibit the moderate enrichment.

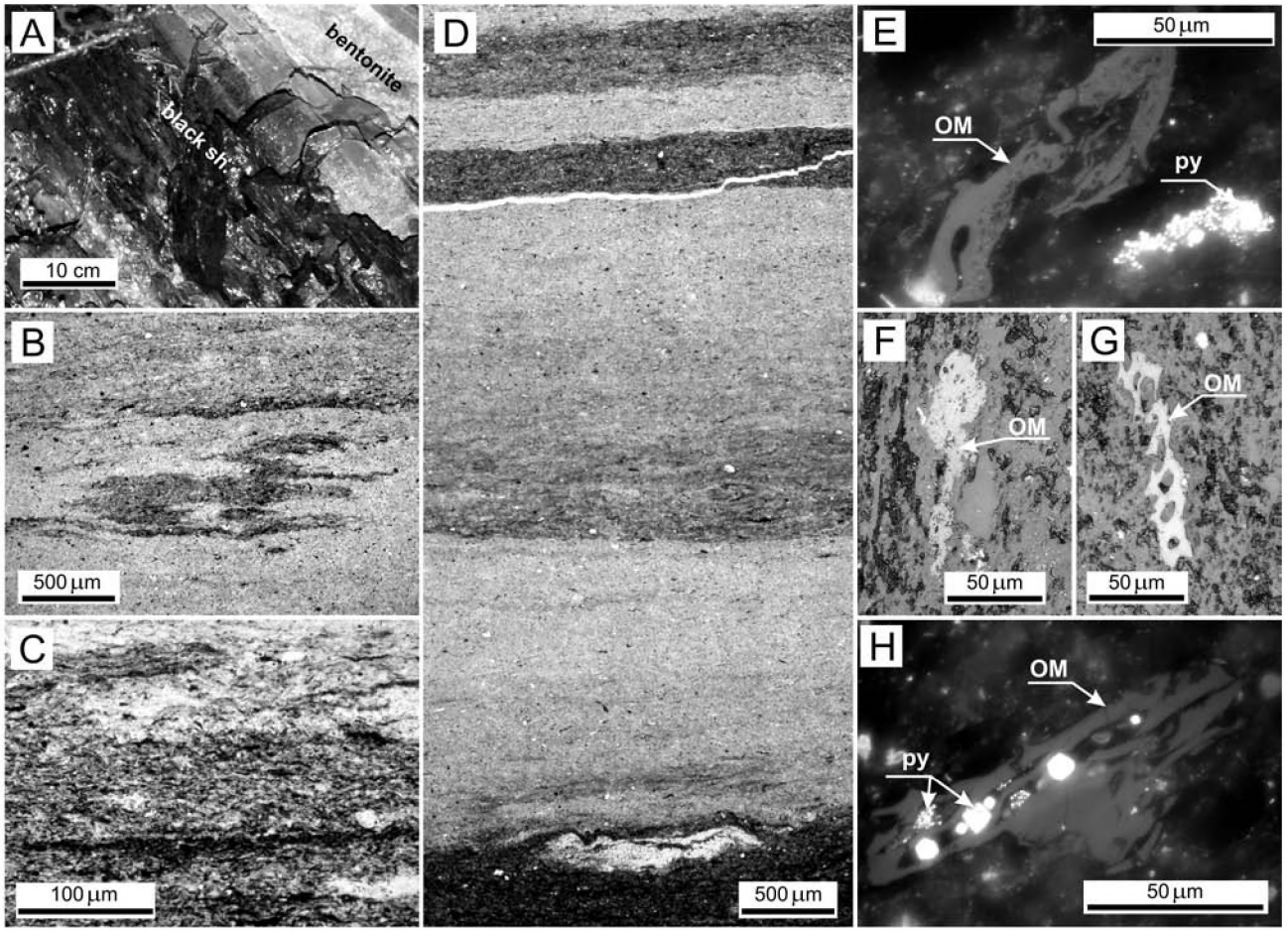

Fig. 5. Middle part of the Barnasiówka Radiolarian Shale Formation in the Lanckorona section; **A.** Non-calcareous black and green shales with yellowish volcanoclastic layer; **B.** Ichnofossils within green shales (LC 5 G sample, TL, II nicols); **C.** Microfacies of parallel-laminated black siliceous shale including detritic grains (LC 5B sample, TL, II nicols); **D.** Parallel lamination and passage from green to black shales (LC 5G sample, TL, II nicols); **E–H.** Organic particle – vitrinite maceral (OM), pyrite (PY; LC 5B sample, RL)

K_2O and large ion lithophile trace elements: Rb, Pb

The percentage of K_2O and Rb varies in broad extent. Most of samples are just below PAAS. Therefore, the samples have enrichment factors below unity (Fig. 9). The ?volcanoclastic sediments of the BRSF contain the highest amounts of K_2O and Rb and display the strongest similarity to PAAS. In contrast, the manganiferous LC 4BG and LC 1 samples represent the poorest sediment. They seem to be relatively enriched in K_2O and Rb (EF >1), but it is a result of low Al_2O_3 content. In general, the K_2O contents correlate with Rb (r^2 equals 0.9) and K_2O/Rb ratio is constant – it amounts to 0.02, like PAAS (Fig. 12).

The lead distribution through the section is irregular. Except of black shale, underlying Mn horizon from the BRSF, the Pb contents are rather low. Cooper and vanadium contents follow this pattern. The enrichment factor for Pb, Cu and V exceed the highest values in the same samples (LC 4B and LC 4BG).

Moreover, correlation between Pb, Cu, V frequency and concentration of organic matter (OM) and S has been recognized (Fig. 10). The samples enriched of OM and/or S contain higher amounts of metals.

Fe_2O_3, MgO, and S-related trace elements: Ag, As, Cd, Co, Cu, Mo, Ni, Se, V, Zn

The average amounts of MgO are low in the Lhoty Formation and higher in the upper part of the section. Within the BRSF and Variegated Shales, the amounts of MgO differ between 0.8 and 2.56%. The manganiferous samples (LC 4 BG and LC 1) contain the lowest amount of MgO, while in the volcanoclastics (LC BT and LC 5G) percentage of MgO is the highest. Finally, the enrichment factor closes to unity in the Lhoty Formation and slightly passes 1 in the upper part of the section (BRSF and Variegated Shales; Fig. 10).

The distribution of the absolute content and enrichment factors for Fe_2O_3 is analogous. The values increase upward to spike in the manganiferous sample (EF is 4.8) and decrease again below 1 in upper BRSF/Variegated Shales.

The absolute contents of S-related elements vary along the section erratically. The Lhoty Formation samples are poor in S and contain small amounts of Ni, Co, Zn, Mo as well. Their enrichment factor does not exceed unity (Fig. 10). Vanadium contents are close to these for PAAS. Only copper concentrations are higher with respect to PAAS.

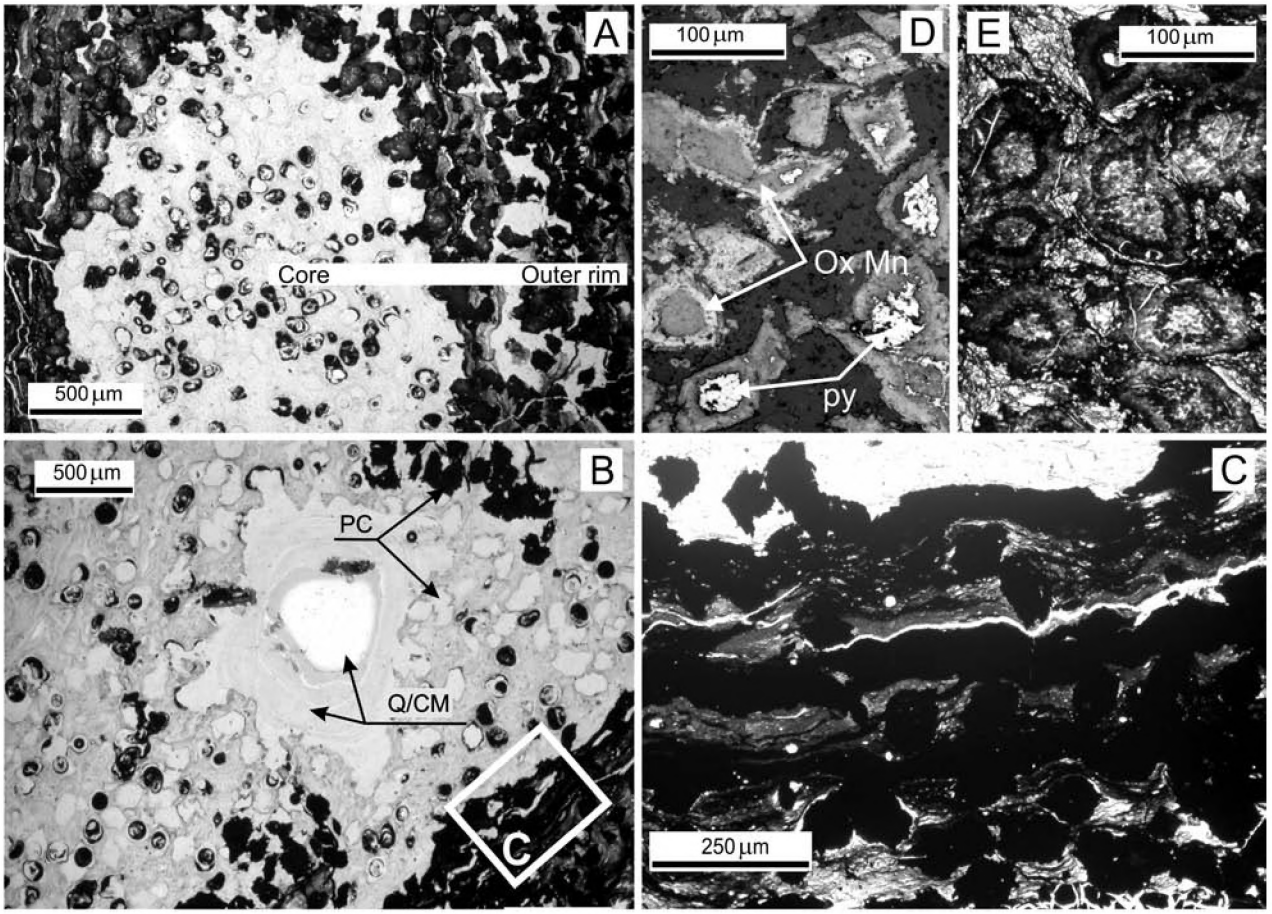

Fig. 6. The ferromanganese horizon overlying the organic-rich facies within the Barnasiówka Radiolarian Shale Formation in the Lanckorona section; sample LC 4 BG; **A.** Fragment of a small-sized ellipsoidal Fe-Mn nodule containing green core and black, outer rim; **B.** Internal core consisting of silica and pseudomorphs after carbonate crystals (PC); matrix composed of clay minerals admixed with silica (Q/CM), TL; **C–E.** Outer rim of nodule including Fe-Mn oxy-, hydroxide (ox Mn) pseudomorphs after carbonates, TL; D. Pseudomorphs containing pyrite (py)

The samples from the BRSF are significantly enriched in V, Co, Ni, Cu, Zn and Mo (Se, As, Cd). This formation consists of OM-rich black shales, where trace element might be trapped by OM and S. The enrichment in Co, Ni, (Ag, Cd) was noted in the manganiferous sample LC 4BG, barren of S (Fig. 10). The enrichment in Co, Mo, Zn, Ni, As, Se occurring in the bentonite sample (LC BT) correlates with presence of S.

In the Variegated Shales, contents of trace elements and S diminish again. They resemble samples of the Lhoty Formation.

TiO_2 and high strength field trace elements: Zr, Nb, Th and Ga

Absolute contents of TiO_2 in the samples studied are generally lower than those for PAAS, thus enrichment factors for TiO_2 are usually below unity (Fig. 11). In detail, the Lhoty Formation samples consist of higher amounts of TiO_2 that decrease upward the succession. Surprising is the peak for LC BT. The minimal percentage was noted in the manganiferous samples of the BRSF (LC 4BG) and VS (LC 1). The second one is sandstone impoverished of Al_2O_3, thus it shows relatively high EF about 1. The behaviour of TiO_2 is similar to Nb and Th, and partly correlates with zircon. The LC 1 sample is extremely enriched due to both high amount of Zr and low amount Al_2O_3.

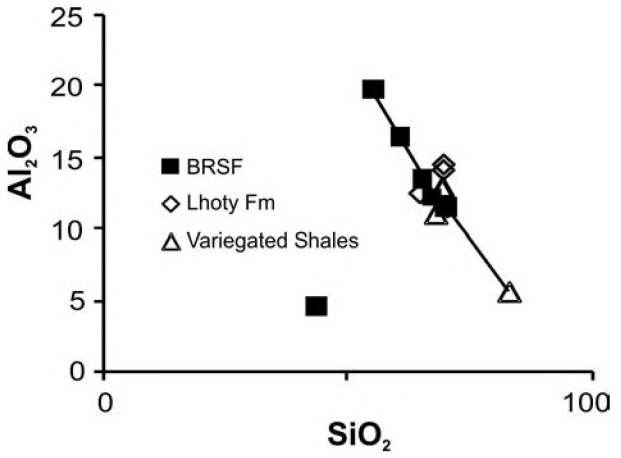

Fig. 7. SiO_2 vs. Al_2O_3 relations in the studied samples from the Lanckorona area. LC 4 BG sample of BRSF is displaced from the curves due to low amounts of oxides and high content of MnO

Table 1

Major and trace element chemistry for the Albian–Lower Turonian sediments from the Lanckorona area, Silesian Nappe

Element	SiO_2	Al_2O_3	Fe_2O_3	MgO	CaO	Na_2O	K_2O	TiO_2	P_2O_5	MnO	S	Th	U	V	Zr	Y	La	Ce
Samples	%	%	%	%	%	%	%	%	%	%	%	ppm	ppm	ppm	ppm	ppm	ppm	ppm
LCL 1	64.84	12.58	3.26	1.3	4.08	0.22	2.7	0.64	0.09	0.03	<0.01	10.1	3.1	120	125.9	16.3	28.6	45.8
LC L 2	69.8	14.2	2.65	1.07	0.93	0.2	2.37	0.54	0.06	0.01	<0.01	11.4	2	101	83.9	13.2	23.9	46
LCL 3	69.84	14.59	2.56	1.14	0.72	0.21	2.42	0.57	0.05	0.02	0.01	11.3	2.1	97	98.3	14.8	25	51.7
LC 7	64	18	3.2	1.23	0.5	0.3	3.4	0.71	0.07	0.03	0.03	13.2	2.4	119	122.6	16.7	28	57.5
LC 6	66.17	16.3	3.9	1.3	0.5	0.3	3.03	0.6	0.08	0.04	0.01	13.2	1.9	114	99.9	17.1	24.5	52.7
LC 5B	70.48	11.52	3.41	1.75	0.73	0.23	2.46	0.42	0.13	0.04	0.43	8.6	3.1	196	61.9	23.8	24.4	59.1
LC 5G	60.8	16.56	5.07	2.56	0.78	0.28	3.63	0.59	0.1	0.04	0.47	13.1	4	175	82.9	21.1	31.4	73.7
LC 5M	67.4	12.26	4.75	1.79	0.49	0.23	2.7	0.45	0.13	0.03	1.25	10	4	263	66.9	24.4	27.5	64.6
LC 4BG	43.82	4.66	7.67	0.72	0.28	0.08	1.41	0.15	0.21	26.6	0.01	3.3	2.9	134	25.6	39	31.4	125.3
LC 4B	65.4	13.54	4.75	1.99	0.71	0.21	3.22	0.5	0.18	0.27	0.01	11.5	2.4	705	71.3	33.7	34.9	74.2
LC BT	55.23	19.9	5.04	2.5	0.77	0.28	4.05	0.78	0.09	0.05	0.31	16.5	4.8	207	108.4	26.3	39.2	87.4
LC 3G	68.23	11.01	2.53	1.57	3.22	0.18	2.39	0.44	0.09	0.13	0.01	8.6	1.8	78	80.1	19.8	27.2	64.6
LC 3B	69.54	12.9	3.35	1.89	0.8	0.24	2.83	0.51	0.09	0.07	0.01	8.7	1.8	137	73.5	20	26.5	60.8
LC 2B	69.49	12.74	2.91	1.77	0.78	0.22	2.64	0.52	0.07	0.08	0.01	10.1	1.7	93	77.6	14.8	25.7	49.5
LC 1	83.06	5.59	2.96	0.82	0.68	0.56	1.04	0.31	0.21	0.7	0.01	8.6	2.4	42	262.7	35	29	72.7

Element	Ba	Co	Ga	Nb	Rb	Ba	Mo	Cu	Pb	Zn	Ni	As	Cd	Ag	Se	Cr
Samples	ppm	ppm	ppm	ppm	ppm	ppm	ppm	ppm	ppm	ppm	ppm	ppm	ppm	ppm	ppm	ppm
LCL 1	313.8	10.4	12.8	13.6	109.1	313.8	0.4	55.2	14.5	45	33.1	4.7	0.1	<0.1	<0.5	90
LC L 2	244.5	6.6	17.1	10.9	94.2	244.5	0.4	100.2	20.3	42	20	3.7	<0.1	<0.1	0.5	70
LCL 3	241.3	6.2	16.7	11.1	97.4	241.3	0.2	100	17.2	44	18.5	1.7	<0.1	0.1	<0.5	70
LC 7	364.7	6.4	3.7	14.7	142.2	364.7	0.1	52.2	18.2	36	19.8	32	0.1	0.1	<0.5	82
LC 6	259.3	11.4	19.8	14.1	119.6	259.3	0.2	129.5	25.2	62	50.8	5.1	0.9	0.1	<0.5	82
LC 5B	275.6	12.4	17.7	7.7	101.7	275.6	1.7	151.9	20	240	52.8	10.1	2	0.8	4	100
LC 5G	293.7	24.7	24.7	12.3	160.7	293.7	0.4	92	24.1	193	89.7	16.9	0.6	<0.1	1.3	90
LC 5M	316.1	18.1	19	9.2	122.8	316.1	10.6	182	25.8	1346	59.6	28.4	4.3	1.2	12.7	110
LC 4BG	3098.9	91.7	31.2	2.7	65.2	3098.9	12.6	290.1	53.8	663	238.3	8.7	4.2	14.5	0.8	30
LC 4B	343.1	20.1	19	10.1	130.9	343.1	0.3	818.8	123	35	46.9	0.8	0.1	0.3	1	110
LC BT	321.5	25.5	23	16.8	168.9	321.5	1.9	123.2	25.2	448	147.5	16.4	0.9	<0.1	6.2	110
LC 3G	316	11	16.9	10.1	117.4	316	<0.1	95.2	10	58	31.9	2.4	<0.1	<0.1	<0.5	70
LC 3B	255.3	20.9	14.8	9	106.5	255.3	<0.1	113.9	22.9	86	36.7	2.7	0.1	0.3	<0.5	80
LC 2B	290.8	22.2	16.2	10.5	111.8	290.8	0.1	57.2	13.8	49	34.8	8.5	<0.1	<0.1	<0.5	70
LC 1	306.8	8.3	7.2	5.7	43.6	306.8	0.9	14.9	10.5	32	23.5	2.2	0.1	<0.1	<0.5	40

<0.1 or <0.5 – below detection limit

The Ga pattern is more irregular (Fig. 11). The highest enrichment (EF=6.34) is measured in the manganiferous shale, whereas the rest of samples display enrichment factor just above 1.

DISCUSSION

PROVENANCE OF THE MINERAL AND ORGANIC DETRITUS

The most important problem is to separate the detrital material from the products of diagenesis and organic supply. The shales in the turbidite succession (Lhoty Formation) contain a relatively small amount of organic matter representing mainly land-originated vitrinite macerals. Glauconite and quartz grains are the second most frequent and unquestionable type of redeposited material. The sorting and addition of biogenic silica may significantly affect the SiO_2/Al_2O_3 ratio, which is used as provenance interpretation (Roster & Grapes, 1990). A value of Si/Al ratio of about 3 is considered to be an average ratio for terrigenous sediments. Values greater than 3 are thought to be due to an "excess" silica supply, probably of biogenic origin (Arthur & Premoli-Silva, 1982). Except of ?bentonite (LC BT sample), the studied samples display values of Si/Al ratio higher than 3. Extremely high ratio was estimated for siliceous LC 1 sample of the Variegated Shales and Mn-rich LC 4 BG

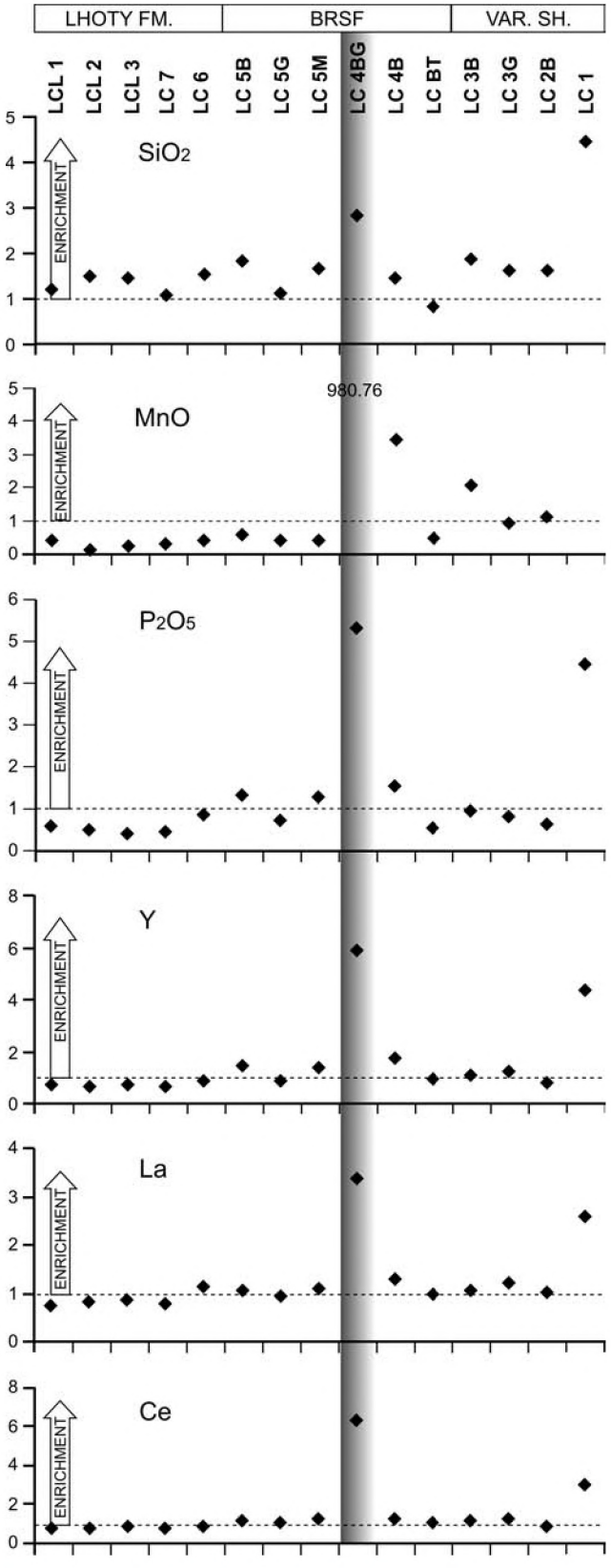

Fig. 8. PAAS-normalised concentrations of SiO_2, MnO, P_2O_5, Y, La, Ce in the studied samples. Dashed line corresponds to PAAS (Taylor & McLennan, 1985)

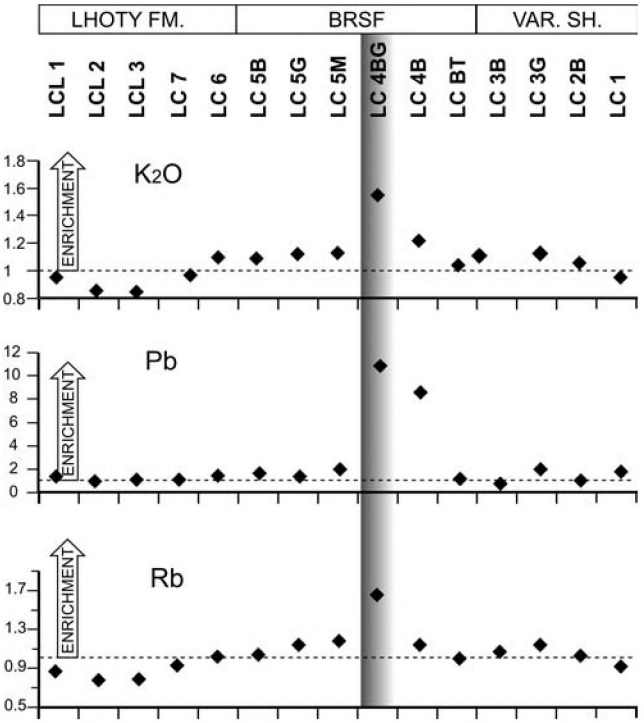

Fig. 9. PAAS-normalised concentrations of K_2O and large ion lithophile trace elements: Rb, Pb in the studied samples. Dashed line corresponds to PAAS (Taylor & McLennan, 1985)

sample. The higher negative correlation may be the effect of predominance of biogenic silica, diluted by terrigenous particles as was earlier suggested by Bąk (2007a, b) for the BRSF in the Silesian, Subsilesian and Skole units. The presence of siliceous tests and detritic quartz in the studied samples was confirmed by thin section observation.

Basing on the absolute contents, the silica is associated with the highest amounts of TiO_2, Nb, Th and Zr. The concentrations of TiO_2, Zr, Nb, Th and Ga, considered to be immobile elements, vary mostly as a function of biogenic dilution in marine sediments and thus are interpreted to be largely detrital (Plank & Langmuir, 1998).

With respect to PAAS, the studied material is poor in TiO_2, Nb and Zr. Two samples only (LC 6, LC 1) are enriched in TiO_2, Nb and Zr that correlate with enhanced frequency of detrital quartz. The amounts of Th and Ga in the studied samples are similar to PAAS. Additionally, the manganiferous LC 4BG sample is extremely enriched in Ga. Most of samples display enrichment factor just above 1, testifying to the small supply of detrital material.

According to Bąk (2007b), an increase in fine detrital input to the Carpathian basin occurred during latest Cenomanian. It is marked by positive excursions of Al/(Al+Fe+Mn) and Rb/Al profiles (Machhlour *et al.*,1994; Wehausen & Brumsack, 1998). The fluvial input was dominating, while the aeolian input might have been negligible, as expressed by the low ratio of Ti/Al (Wehausen & Brumsack, 1998). The share of land-derived siliciclastic material was fairly constant during the Cenomanian–Turonian Boun-dary (CTB) interval.

Plank and Langmuir (1998) have showed strong correlation between trace elements, including alkalis (K, Rb) and

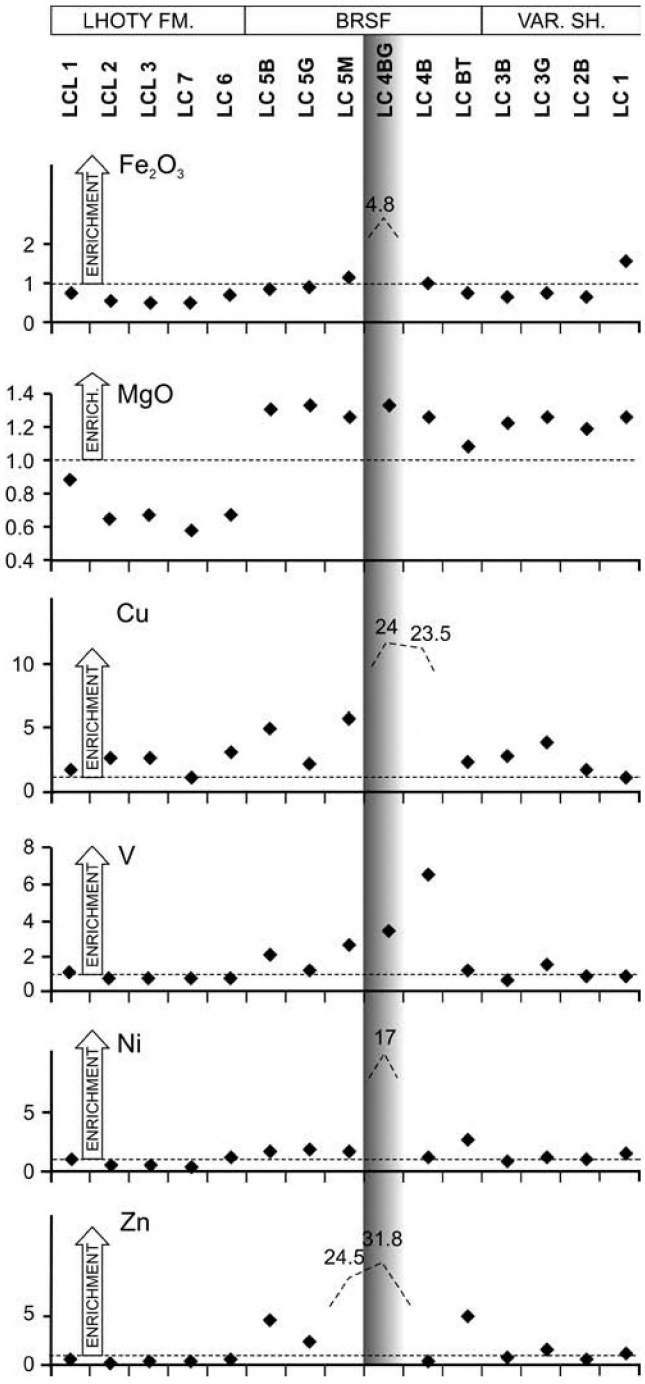

Fig. 10. PAAS-normalised concentrations of Fe_2O_3, MgO, and trace elements: V, Ni, Cu, Zn in the studied samples. Dashed line corresponds to PAAS (Taylor & McLennan, 1985)

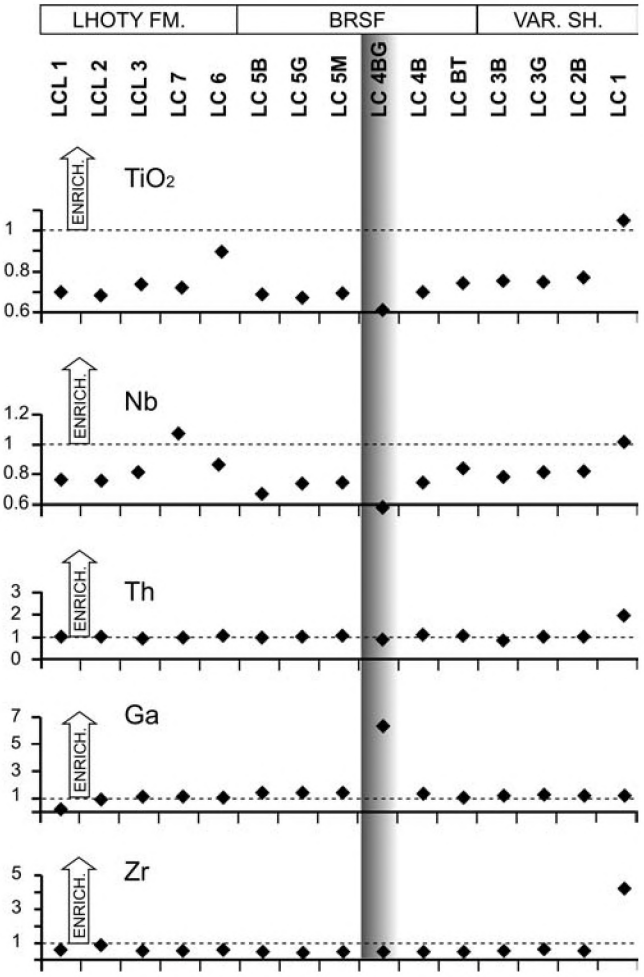

Fig. 11. PAAS-normalised concentrations of TiO_2 and high strength field trace elements: Zr, Nb, Th and Ga in the studied samples. Dashed line corresponds to PAAS (Taylor & McLennan, 1985)

lithology, and that their ratios are predominantly due to continental input. Contributions from volcanic sources can be estimated using the K_2O/Rb ratio (Fig. 12). Low K_2O/Rb ratios are typical of weathered sources (McLennan *et al.*, 1990), whereas high K_2O/Rb ratios are characteristic of sediments rich in volcanoclastics or sediments that have been altered due to K metasomatism (Plank & Languir, 1998). The investigated samples have the K_2O/Rb ratio similar to detritus derived from the upper continental crust (Chester, 1990; Fig. 12).

The continental affinity of the studied samples can be tested using the Y/Ni and Cr/V elemental ratios, which are used to identify mafic sources (Hiscott, 1984). The studied samples are very similar to PAAS (Fig. 13). However, a mafic-ultramafic contribution can be excluded. Andreozzi *et al.* (1997) have proposed a diagram basing on the contents of some transition metals (V, Ni, Cr) and immobile elements (Zr and Ti) to discriminate a possible volcanoclastic or terrigenous contribution. The samples investigated plot within the terrigenous field (Fig. 14).

These data correspond with earlier paradigm that siliciclastic particles were supplied to the Outer Carpathian basins from the European Platform (*e.g.*, Wieser, 1948; Burtan *et al.*, 1984; Bąk, 2007 b).

The high content of silica may indicate relative increase in organic productivity in the latest Cenomanian–earliest Turonian times. The numerous radiolarian-rich layers probably reflect upwelling circulation at the margin of the Carpathian Basin (Bąk, 2006, 2007 a, b). The abundance of radiolarians is linked to the marine organic matter enrichment.

The amorphous macerals in the black shales of the BRSF were identified as colovitrinite and altered bitu-

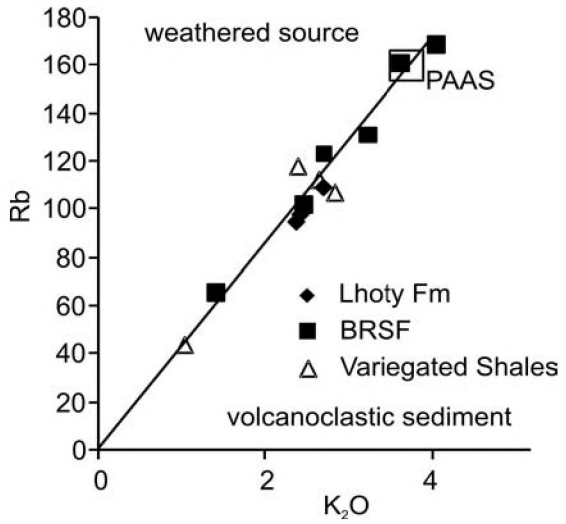

Fig. 12. K_2O vs. Rb diagram. The values of K_2O/Rb ratio in the studied samples are similar to that of the PAAS (McLennan *et al.*, 1990)

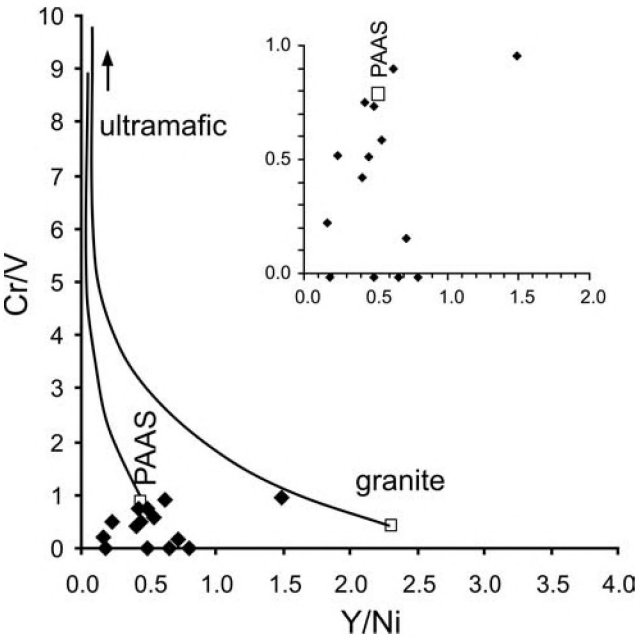

Fig. 13. Cr/V vs. Y/Ni diagram. Ultramafic sources have low Y/Ni and high Cr/V ratio, contrary to granitic where Y/Ni is high and low Cr/V ratio. Samples are distributed close to the PAAS end-member

minite. The source material of bituminite is predominantly phytoplanctonic and bacterial. To lower extent the bituminite is derived from zooplankton, cyanobacteria and other organic material (International Committee for Coal Petrology, ICCP, 1993; Tyson, 1995).

The changed proportion of land to marine organic matter was directly resulted by eustatic sea level rise, with maximum in the earliest Turonian (Jacquin *et al.*, 1998). This event has caused a decrease in supply of siliciclastic material to the Tethyan marginal basins and could promote increased nutrient supply to surface waters that would have supported increased productivity in epicontinental seas and marginal deep basins (*cf.* Bąk, 2007c).

The black shales of the BRSF display high concentration of Cd, Zn, V, Mo, Ag, As. An explanation of this phenomenon could be marine-origin of the organic matter. Biophile elements are absorbed by organisms and scavenged to sediment by organic matter. Cd, Ag and Se correlate with nutrient elements in sea-water and can accumulate in the sediment primarily bound to organic carbon (Ndung'u *et al.*, 2001; Bruland, 1980). The black shales of the Bonarelli-equivalent level analysed by Bąk (2007 a, b, c) reveal high values of the As/Al ratio. The author postulated that part of organic matter could be of algae-derivation. Arsenic is absorbed by planktonic organisms (mainly by algae) and accumulated within organic matter (Francesconi & Edmonds, 1998 in Bąk, 2007 c).

Cd and Ag as sulphide-forming metals can form the stable sulphides (Jacobs *et al.*, 1985). The studied samples are S enriched as well. It is possible, that S-related trace-elements could be incorporated into sediment during precipitation of sulphides.

The mineral composition of the studied clay material is correlative with other Cretaceous samples. Robert and Chamley (1982) suggest that the clay-mineral composition of the Cretaceous oceanic sediments is rather a function of the primary source input. These authors came to the conclusion that illite and chlorite were detrital in origin and indicate the periods of intense physical erosion, whilst smectite might evidence climatic condition or volcanic activity suitable for neoformation of clay minerals (Chamley, 1989). In Spain, the Early Cretaceous succession are rich in kaolinite and illite. High amount of kaolinite suggests that the deposit was formed under warm, wet condition favourable to chemical wathering of acidic rocks. Towards the top, the amount of smectite increases gradually. The increase in smectite indicates influence of the Cenomanian transgression (Chamley, 1989).

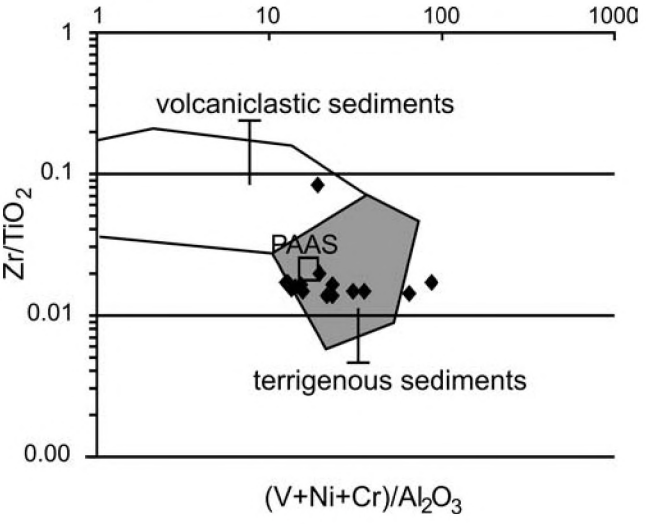

Fig. 14. Discrimination diagram (Andeozzi *et al.*, 1997) showing that the samples are mostly derived from terrigenous supply

Clay mineral composition of the investigated samples suggests that the Lhoty Formation is enriched in illite and kaolinite, probably terrigenous-derived, whereas the shales of the BRSF consist mainly of smectite-rich phases. Mineral composition of the bentonites in the CTB interval succession has been studied by Koszarski *et al.* (1962), Burtan & Turnau-Morawska (1978), and Bąk (2006). They exhibit analogous petrology and describe the same igneous provinces.

Hoffman and Hower (1979) have proposed smectite percentage in illite-smectite in shales to be a palaeogeothermometer. They concluded the onset of illitisation at 60°C, therefore high share of smectite in the investigated illite – smectite might indicate a low-temperature diagenesis.

DIAGENESIS

The diagenetic processes have affected the sediment studied. They are evidenced by alteration of organic matter, as well as geochemical (relation between REE, Mn, P_2O_5) and mineralogical (pyrite and clay minerals, ferromanganese nodules) imprints.

During diagenesis, the bituminite material becomes thin banded or fine grained and increasingly vitrinite-like (metabituminite after Teichmüller & Ottenjann, 1977 and micrinite after ICCP, 1993). The metabituminite might be more accurate for the characterization of the coalification residues of bituminite. Such macerals were interpreted by Stasiuk (1993) as products of degradation and microbial alternation of marine organic matter, both within the water column and the sediment.

The high REE concentrations might be a combined effect of the occurrence of Mn-oxyhydroxides (MnO-rich sediments scavenge Ce^{4+}) and fish debris (high P_2O_5 sediments inherit negative Ce anomalies) in the areas of slow pelagic sedimentation (Plank & Langmuir, 1998; Reynard *et al.*, 1999). None of the above processes have affected the analysed sediment. Consequently, REE were redistributed in sediments during diagenesis (Rasmussen, 1996; Rasmussen *et al.*, 1998; Lev *et al.*, 1998, 1999) and this overprint is related with the presence of secondary minerals, such as phosphates and sulphur minerals. It seems to be the most probable explanation for LC 5B and LC 5M samples that are MnO depleted but enriched in REE, P_2O_5 and S.

Diagenetic origin of the ferromanganese nodules was presented by Bąk (2006, 2007a–d). Some chemical indices of the Fe-Mn layers were studied in detail in the representative sections of the Subsilesian and Skole nappes. The first Fe-Mn layer displays features of hydrogenous to diagenetic sediment, while the second one has features of hydrothermal deposit (Bąk, 2007 c, d).

Pyrite in the internal part of rhomboedric pseudomorphs occurs as massive, irregular aggregates. Large octahedral crystals (average 20 μm in diameter) appear within the light-coloured samples. They precipitated in sediments underlying oxic water column (diagenetic; Wignall & Newton, 1998). Contrary to thin framboidal (up to 10 μm in diameter) pyrite within the black shales. Framboids that are on the average smaller and less variable in size was formed in the euxinic water column (syngenetic; Raiswell & Berner, 1985; Wignall & Newton, 1998).

CONCLUSIONS

The major and trace element geochemistry of the siliciclastic and hemipelagic sediments of three lithostratigraphic units: Lhoty Formation, Barnasiówka Radiolarian Shale Formation and Variegated Shales from Lanckorona area, Polish Outer Carpathians suggests a largely continental source. A biogenic siliceous source is recognised for the portion of the Lhoty Formation and the BRSF of the studied succession. The input of marine organic matter into deposits of the middle part of BRSF is very important as well. Therefore, it can be concluded that the supply of material to the clay- rich layers of the Lhoty Formation, BRSF and Variegated Shales sampled in the Lanckorona area are mainly derived from two major inputs. The first is a dominant terrigenous fine-grained component, having affinity with the average upper continental crust. The second component of the source is a marine-derived biogenic material (silica and organic substances – metabituminite).

The studied sediment was diagenetically altered. The following data are evidencing these conclusions: coalification of bituminite, low-temperature illitisation of smectite, precipitation of secondary minerals such as phosphates and sulphides, formation of ferromanganese nodules.

Acknowledgements

Krzysztof Bąk (Pedagogical University), Zbigniew Sawłowicz (Jagiellonian University) and Jan Golonka (AGH University of Science and Technology) are thanked for valuable discussion and comments on the manuscript. Wojciech Narębski (Museum of the Earth) is acknowledged for improving the English and Leszek Chudzikiewicz (Institute of Geological Sciences, Polish Academy of Sciences, Kraków) for help with editorial remarks. This work was financially supported by a grant of the Polish Ministry of Scientific Research and Information Technology no. 2P04D 080 29.

REFERENCES

Andreozzi, M., Dinelli, E. & Tateo, F., 1997. Geochemical and mineralogical criteria for the identification of ash layers in the stratigraphic framework of a foredeep; the early Miocene Mt. Cervarola sandstones, northern Italy. *Chemical Geology*, 137: 23–39.

Arthur, M.A., Premoli Silva, I., 1982. Development of widespread organic carbon-rich strata in the Mediterranean Tethys. In: Schlanger, S.O., Cita, M.B. (Eds.), *Nature and Origin of Cretaceous Carbon-Rich Facies*. Academic Press, London, pp. 7–54.

Bąk, K., 2006. Sedimentological, geochemical and microfaunal responses to environmental changes around the Cenomanian–Turonian boundary in the Outer Carpathian Basin; a record from the Subsilesian Nappe, Poland. *Palaeogeography, Palaeoecology, Palaeoclimatology*, 237: 335–358.

Bąk, K., 2007a. Deep-water facies succession around the Cenomanian–Turonian boundary in the Outer Carpathian Basin: high-resolution sedimentary, biotic and chemical records in the Silesian Nappe, Poland. *Palaeogeography, Palaeoecology, Palaeoclimatology*, 248: 255–290.

Bąk, K., 2007b. Environmental changes around the Cenomanian–Turonian boundary in a marginal part of the Outer Carpathian Basin expressed by microfacies, microfossils and chemical records in the Skole Nappe (Poland). *Annales Societatis Geologorum Poloniae*, 77: 39–67.

Bąk, K., 2007c. Environmental changes during the Cenomanian–Turonian Boundary Event in the Outer Carpathian Basins: a synthesis of data from various tectonic- facies units. *Annales Societatis Geologorum Poloniae*, 77: 171–191.

Bąk, K., 2007d. Organic-rich and manganese sedimentation during the Cenomanian–Turonian boundary event in the Outer Carpathian Basin; a new record from the Skole Nappe, Poland. *Palaeogeography, Palaeoecology, Palaeoclimatology*, 256: 21–46.

Bąk, K., Bąk, M. & Paul, Z., 2001. Barnasiówka Radiolarian Shale Formation – a new lithostratigraphic unit in the Upper Cenomanian–lowermost Turonian of the Polish Outer Carpathians (Silesian Series). *Annales Societatis Geologorum Poloniae*, 71: 75–103.

Bąk, M., Bąk, K. & Ciurej, A., 2005. Mid-Cretaceous spicule-rich turbidites in the Silesian Nappe of the Polish Outer Carpathians: radiolarian and foraminiferal biostratigraphy. *Geological Quarterly*, 2005, 49: 275–290

Bieda, F., Geroch, S., Koszarski, L., Książkiewicz, M. & Żytko, K., 1963. Stratigraphie des Karpates externes polonaises. *Biuletyn Instytutu Geologicznego*, 181: 5–174.

Bruland, K. W., 1980. Oceanographic distribution of cadmium, zinc, nickel and copper in the North Pacific. *Earth and Planetary Science Letters*, 47: 176–198.

Burtan, J. & Turnau-Morawska, M., 1978. Biochemical siliceous rocks of the West Carpathian Flysch. *Prace Geologiczne. Polska Akademia Nauk, Oddział w Krakowie*, 111: 1–36.

Burtan, J., Chowaniec, J.& Golonka, J., 1984. Preliminary results of studies on exotic carbonate rocks in the western part of the Polish Flysch Carpathians (in Polish with English and Russian summaries). *Biuletyn Instytutu Geologicznego*, 346: 147–155.

Chamley, H., 1989. *Clay sedimentology*, Springer-Verlag, Berlin, 623 pp.

Chester, R., 1990. *Marine Geochemistry*, Chapman and Hall, London, 698 pp.

Dudek, T. & Środoń, J., 1996. Identification of illite/smectite by X-ray powder diffraction taking into account the lognormal distribution of crystal thickness. *Geologica Carpathica - Series Clays*, 5: 21–32.

Gedl, E., 2001. The latest Albian–Cenomanian age of the Lgota Beds from the Rzyki quarry (Silesian Nappe, Polish Flysch Carpathians) on the basis of dinocyst study. *Biuletyn Państwowego Instytutu Geologicznego*, 396: 49–50.

Geroch, S., Gucwa, I. & Wieser, T., 1985. Manganese nodules and other indications of regime and ecological environment in lower part of the Upper Cretaceous — exemplified by Lanckorona profile. In: Wieser, T. (ed.), *Fundamental Researches in the Western Part of the Polish Carpathians, 13th Congress of Carp.—Balk. Geol. Assoc., Guide to Excursion I*, Geol. Inst., Cracow, pp. 88–100.

Golonka, J., Oszczypko, N. & Ślączka, A., 2000. Late Carboniferous – Neogene geodynamic evolution and paleogeography of the circum-Carpathian region and adjacent areas. *Annales Societatis Geologorum Poloniae*, 70: 107–136.

Golonka, J., Krobicki, M., Waśkowska-Oliwa, A., Słomka, T., Skupien, P, Vašíček, Z., Cieszkowski, M. & Ślączka, A., 2008a. Lithostratigraphy of the Upper Jurassic and Lower Cretaceous deposits of the western part of Outer Carpathians (discussion proposition). (In Polish, English summary). In: Krobicki, M. (ed.), *Utwory przełomu jury i kredy w zachodnich Karpatach fliszowych polsko-czeskiego pogranicza. Kwartalnik AGH, Geologia*, 34(3/1): 9–31.

Golonka, J., Krobicki, M., Waśkowska-Oliwa, A., Vašíček, Z. & Skupien P, 2008b. Main paleogeographical elements of the West Outer Carpathians during Late Jurassic and Early Cretaceous times. (In Polish, English summary). In: Krobicki, M. (ed.), *Utwory przełomu jury i kredy w zachodnich Karpatach fliszowych polsko-czeskiego pogranicza. Kwartalnik AGH, Geologia*, 34(3/1): 61–72.

Gucwa, I. & Wieser, T., 1978. Ferromanganese nodules in the Western Carpathian flysch deposits of Poland. *Annales Societatis Geologorum Poloniae*, 48: 147–182.

Hiscott, R. N., 1984. Ophiolitic source rocks for Taconic-age flysch: trace-element evidence. *Geological Society of America Bulletin*, 95: 1261–1267.

Hoffman, J. & Hower, J., 1979. Clay mineral assemblages as low grade metamorphic geothermometers: application to the thrust-faulted disturbed belt of Montana, U.S.A. In: J. Slater & J. Schluger (eds), *Diagenesis. SEPM Special Publication*, 26: pp. 55–79.

International Committee for Coal Petrology, ICCP, 1993. Bituminite in Rock Other than Coal. *International Handbook of Coal Petrology*. 3rd suppl. 2nd ed., Newcastle, 15 pp.

Jackson, M.L., 1975. *Soil Chemical Analysis – Advanced Course.* Published by the author, Madison, Wisconsin.

Jacquin, T.& de Graciansky, P. C., 1998. Major transgressive/regressive cycles: the stratigraphic signature of European Basin development. In: de Graciansky, P. C. *et al.* (eds), *Mesozoic and Cenozoic Sequence Stratigraphy of European Basins. SEPM Special Publication*, 60: 15–29.

Jacobs, L., Emerson, S. & Skei, J., 1985. Partitioning and transport of metals across the O_2/H_2O interface in a permanently anoxic basin: Framvaren Fjord, Norway. *Geochimica et Cosmochimica Acta*, 49: 1433–1444.

Koszarski, L., Książkiewicz, M., Nowak, W., Szymakowska, L. & Ślączka A. 1962. *Rozmieszczenie facji albu, cenomanu w polskich Karpatach zewnętrznych. Atlas Geologiczny Polski.* (In Polish). Instytut Geologiczny. Warszawa

Koszarski, L. & Ślączka, A., 1973. Outer (flysch) Carpathians: Lower Cretaceous. In: Pożaryski, W. (ed.), *Geology of Poland*. Wydawnictwa Geologiczne, Warszawa, pp. 492–495.

Kovač, M., Nagymarosy, A., Oszczypko, N., Ślączka, A., Csontos, L., Marunteanu, M., Matenco, L. & Marton, E., 1998. Palinspastic reconstruction of the Carpathian-Pannonian region During the Miocene, In: Rakus, M. (ed.), *Geodynamic development of the Western Carpathians*. Slovak Geological Survey, Bratislava: 189–217.

Książkiewicz, M., 1951. *Objaśnienia arkusza Wadowice. Ogólna mapa geologiczna Polski 1: 50 000.* (In Polish). Państwowy Instytut Geologiczny, Warszawa, 283 pp.

Książkiewicz, M. (ed.), 1962. *Geological Atlas of Poland, Stratigraphic and facial problems. Fasc.13 – Cretaceous and Early Tertiary in the Polish External Carpathians, 1:600 000.* Instytut Geologiczny, Warszawa.

Książkiewicz, M., 1977. Tectonics of the Carpathians. In: Pożaryski, M. (ed.), *Geology of Poland, Tectonics*. Wydawnictwa Geologiczne, Warszawa, pp. 476–604.

Lev, S. M., McLennan, S. M., Meyers, W. J. & Hanson, G. N., 1998. A petrographic approach for evaluating trace-element mobility in a black shale. *Journal of Sedimentary Research*, 68: 970–980.

Lev, S. M., McLennan, S. M. & Hanson, G. N., 1999. Mineralogical controls on REE mobility during black-shale diagenesis. *Journal of Sedimentary Research*, 69: 1071–1082.

Machhlour, L., Philip, J. & Oudin, J. L., 1994. Formation of laminate deposits in anaerobic – dysaerobic marine environments. *Marine Geology*, 117: 287–302.

Ndung'u, K., Thomas, M. A. & Flegal, A. R. 2001. Silver in western equatorial and South Atlantic Ocean. *Deep-Sea Research II*, 48: 2933–2945.

McLennan, S. M., Taylor, S. R., McCulloch, M. T. & Maynard, J. B., 1990. Geochemical and Nd–Sr isotopic composition of deep-sea turbidites: crustal evolution and plate tectonic associations. *Geochimica et Cosmochimica Acta*, 54: 2015–2050.

Moore, D. M. & Reynolds Jr., R. C., 1997. *X-Ray Diffraction and the Identification and Analysis of Clay Minerals*. Oxford Univ. Press, Oxford. 332 pp.

Nemčok, M., Nemčok, J., Wojtaszek, M., Ludhova, L., Oszczypko, N., Sercombe, W. J., Cieszkowski, M., Paul, Z., Coward, M. P. & Ślączka, A. 2001. Reconstruction of Cretaceous rifts incorporated in the Outer West Carpathian wedge by balancing. *Marine and Petroleum Geology*, 18: 39–64.

Oszczypko, N., 1999. From remnant oceanic basin to collision-related foreland basin – a tentative history of the Outer Carpathians. *Geologica Carpathica*, 50 (special issue): 161–163.

Oszczypko, N., 2004. The structural position and tectonosedimentary evolution of the Polish Outer Carpathians. *Przegląd Geologiczny*, 52: 780–791.

Plank, T. & Langmuir, C. H., 1998. The chemical composition of subducting sediment and its consequences for the crust and mantle. *Chemical Geology*, 145: 325–394.

Poprawa, P., Malata, T. & Oszczypko, N. 2002. Tectonic evolution of the Polish part of Outer Carpathian's sedimentary basins – constraints from subsidence analysis. *Przegląd Geologiczny*, 50: 1092–1108.

Rasmussen, B., 1996. Early-diagenetic REE-phosphate minerals (florencite, gorceixite, randallite, and xenotime) in marine sandstones: a major sink for oceanic phosphorus. *American Journal of Science*, 296: 601–632.

Rasmussen, B., Buick, R. & Taylor, W. R., 1998. Removal of oceanic REE by authigenic precipitation of phosphatic minerals. *Earth and Planetary Science Letters*, 164: 135–149

Raiswell, R. & Berner, R. A., 1985. Pyrite formation in euxinic and semi-euxinic sediment. *American Journal of Science*, 285: 710–724.

Reynard, B., Lécuyer, C. & Grandjean, P., 1999. Crystal-chemical controls on rare-earth element concentrations in fossil biogenic apatites and implications for paleoenvironmental reconstructions. *Chemical Geology*, 155: 233–241.

Robert, C. & Chamley, H., 1982. Paleoenvironmental significance of clay deposits in Atlantic black shales. In: Schlanger, S. O. & Cita, M. B. (eds) *Nature and origin of Cretaceous carbon-rich facies*. Academic Press, London, pp. 101–112.

Roster, B. & Grapes, R., 1990. Geochemistry of a metabasite-chert-coloured argillite-turbidite association at Red Rocks, Wellington, New Zealand. *New Zealand Journal of Geology and Geophysics*, 33, 181–191.

Ślączka, A., Kruglow, S., Golonka, J. Oszczypko, N. & Popadyuk, I, 2006. The General Geology of the Outer Carpathians, Poland, Slovakia, and Ukraine. In: Golonka, J. & Picha, F. (eds.) *The Carpathians and their foreland: Geology and hydrocarbon resources. American Association of Petroleum Geologists, Memoir*, 84: 221–258.

Środoń, J., 1980. Precise identification of illite/smectite interstratifications by X-ray powder diffraction. *Clays and Clay Minerals*, 28: 401–411.

Środoń, J., 1984. X-ray powder diffraction identification of illitic materials. *Clays & Clay Minerals*, 32: 337–349.

Stasiuk, L. D., 1993. Algal bloom episodes and the formation of bitumminite and micrinite in hydrocarbon source rocks: evidence from the Devonian and Mississippian, northern Williston Basin, Canada. *International Journal of Coal Geology*, 24: 195–210.

Taylor, S. M. & McLennan, S. M., 1985. *The continental crust: its composition and evolution.* Blackwell Scientific, Oxford, 312 pp.

Teichmüller, M.,& Ottenjann, K., 1977. Liptinite und lipoide Stoffe in einem Erdölmuttergestein. *Erdöl und Kohle*, 30: 387–398.

Tyson, R. V., 1995. *Sedimentary Organic Matter*. Chapman and Hall, London, 615 pp.

Wehausen, R. & Brumsack, H.-J., 1998. The formation of Pliocene Mediterranean sapropels: constraints from high-resolution major and minor element studies. In: Robertson, A. H. F., Emeis, K.-C., Richter, C. *et al.* (eds), *Proceedings of the Ocean Drilling Program, Scientific Results*, 160, College Station, TX, pp. 207–217.

Wieser, T., 1948. Egzotyki krystaliczne w kredzie śląskiej okolic Wadowic (In Polish, English summary). *Rocznik Polskiego Towarzystwa Geologicznego*, 18: 36–150.

Wignall, P. B. & Newton, R., 1998. Pyrite framboid diameter as a measure of oxygen deficiency in ancient mudrocks. *American Journal of Science*, 298: 537–552.

Żytko, K., Gucik, S., Ryłko, W., Oszczypko, N., Zając, R., Garlicka, I., Nemčok, J., Eliáš, M., Menčik, E., Dvorák, J., Stránik, Z., Rakús, M. & Matejovská, O., 1989. Geological Map of the Western Outer Carpathians and their foreland without Quaternary formations. Scale 1:500 000. In: D. Poprawa, D. & Nemčok, J. (ed.), *Geological Atlas of the Western Outer Carpathians and their Foreland*. Państwowy Instytut Geologiczny, Wydawnictwa Geologiczne, Warszawa